Spectral Functions and Transport in High Temperature QCD

Gert Aarts

Department of Physics, Swansea University, Swansea, UK

I review results on transport coefficients, spectral functions and charmonium in high temperature QCD, obtained using nonperturbative lattice QCD simulations.

§1. Introduction

The relativistic heavy ion experiments at RHIC have made it clear that is important to understand real-time and nonequilibrium processes in the quark-gluon plasma. In this talk I focus on two developments, connected through the construction of spectral functions from lattice QCD correlators: charmonium in lattice QCD with two dynamical fermion flavours at high temperature and transport coefficients and spectral functions at small energies obtained via the Maximum Entropy Method. For more details and much more references I refer to a recent review.[1)]

§2. Charmonium

What happens to heavy quark bound states when they are immersed in a quark-gluon plasma? New answers to this old question emerged a few years ago, mainly due to the analysis of spectral functions, constructed from euclidean lattice correlators using the Maximum Entropy Method (MEM). Spectral function studies of charmonium in quenched lattice QCD indicated that S wave states (J/ψ and η_c) may survive up to temperatures $T \sim 2T_c$, whereas P waves (χ_{c0} and χ_{c1}) melt quickly after the deconfinement transition.[2)–4)] An obvious question is to ask what will happen when the plasma contains quarks as well and is no longer just a gluon plasma. Below I report on work performed in a collaboration between Trinity College Dublin and Swansea addressing this point.[5)]

But first I want to start with a warm-up problem and consider meson correlators in vacuum. The UKQCD and RBC collaborations have recently used the domain wall formulation[6)] of lattice fermions to generate ensembles with $2+1$ flavours of dynamical fermions at zero temperature.[7)] Together with Justin Foley, we have studied lattice spectral functions for chirally symmetric fermions (overlap, domain wall, overlap hypercube) analytically and have performed a MEM analysis of some of the UKQCD/RBC data.[8)] Here I show one result from a spectral study on a lattice of size $16^3 \times 32$, with $N_s = 16$ in the fifth dimension. In Fig. 1 (left) the pseudoscalar spectral function is shown as a function of energy ω, for three combinations of valence quark masses. Clearly visible are the narrow pion groundstate peaks. Also indicated, via the vertical dotted lines, are the groundstate masses obtained with conventional exponential fits. Both methods nicely agree. At larger energies a second broad bump appears. This might be a signal for (a combination of) excited states, but it can

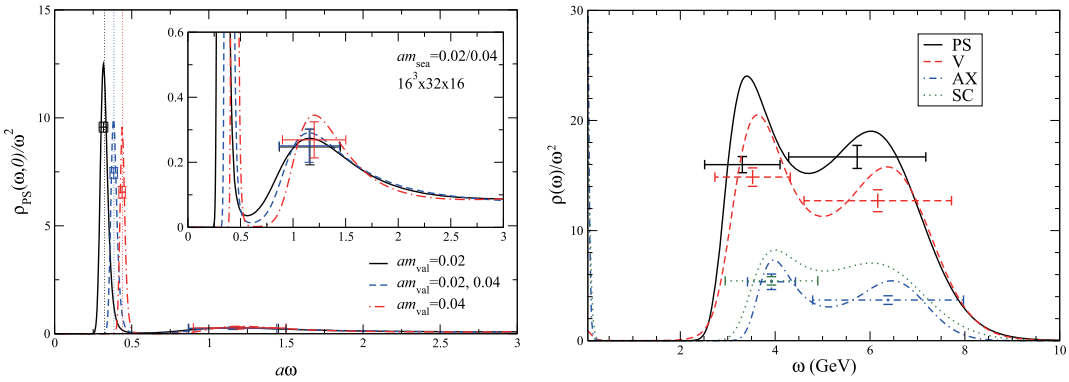

Fig. 1. Left: Pseudoscalar spectral functions in QCD with $2+1$ flavours of dynamical domain wall fermions, for different values of the valence quark masses. The vertical dotted lines indicate groundstate masses obtained with conventional cosh fits. The inset shows a blow-up of the second bump. Right: Charmonium spectral functions just above T_c ($T/T_c = 1.05$) in the pseudoscalar (PS), vector (V), axial-vector (AV) and scalar (SC) channels.

also be a lattice artefact due to the finite Brillouin zone on the lattice. With just one lattice spacing available it is currently not possible to distinguish these options. However, the second possibility is expected from free lattice fermion studies, where structure at energies $1 \lesssim a\omega \lesssim 3$ is found.[8)–10)] It will be necessary to do a similar analysis at a different lattice spacing to resolve this. Note that the lattice spacing is sufficiently small such that the physical groundstate is located at $a\omega \sim 0.4 \ll 1$.

I now turn to the study of charmonium at finite temperature. In order to have a sufficient number of lattice points in the euclidean time direction, mandatory for the application of MEM, highly anisotropic lattices were used. The tuning of the anisotropy is more involved in dynamical simulations compared to quenched calculations.[11)] The ratio between the spatial and temporal lattice spacing $\xi = a_s/a_\tau$ is approximately equal to 6, with $a_s \approx 0.165$ fm. The critical transition takes place at $N_\tau \sim 32.5$ ($T/T_c = 1.05$ at $N_\tau = 32$). Given these parameters it is possible to increase the temperature in steps of $\Delta T \approx 7$ MeV around T_c. The results shown here are obtained on lattices with size $8^3 \times N_\tau$ and $12^3 \times N_\tau$, with $N_\tau = 32, \ldots, 16$ (or $T/T_c = 1.05, \ldots, 2.1$, see Table I). In Fig. 1 (right) the charmonium spectral functions are shown just above T_c in four channels. In this case the separation between the first and second peaks at larger ω is not so clear as in the zero-temperature plot discussed earlier. This is partly due to the coarser lattice used in this study and partly due to being at finite temperature, which makes the MEM analysis more involved. However,

Table I. Relation between temperature T and the extent in the euclidean time direction N_τ in the charmonium study.

N_τ	32	31	30	29	28	24	20	18	16
T/T_c	1.05	1.08	1.12	1.16	1.2	1.4	1.68	1.86	2.1
T(MeV)	221	228	235	243	252	294	353	392	441

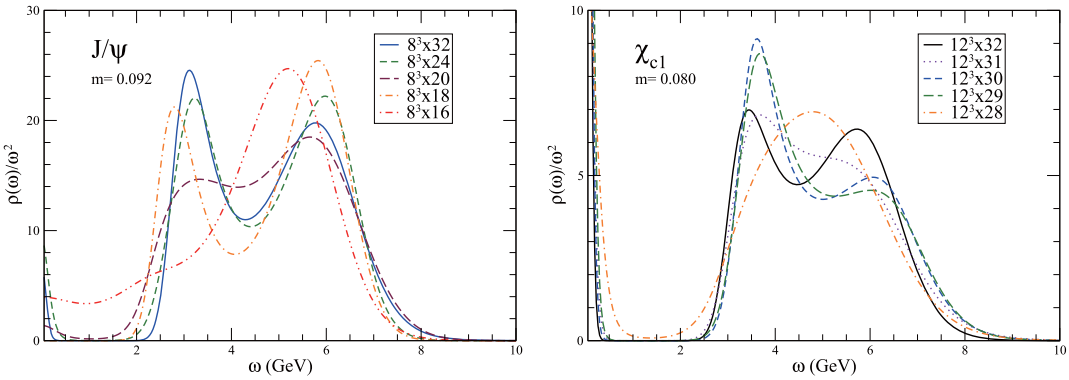

Fig. 2. Pseudoscalar (left) and axial-vector (right) spectral functions at different temperatures.

we are confident that the first peaks are physical, since their positions agree with the groundstate masses obtained at zero temperature (with $N_\tau = 80$).

In Fig. 2 (left) the response in the vector channel (J/ψ) to a hotter environment is shown; the temperatures are $T/T_c = 1.05, 1.40, 1.68, 1.86$ and 2.09. At the two lowest temperatures the peak structure is very similar, while at the highest temperature the groundstate peak has certainly disappeared. At the intermediate temperatures the pattern is not so clear. We conclude therefore that the J/ψ survives to at least $T \sim 1.4T_c$ but has certainly melted at $T \sim 2T_c$. In Fig. 2 (right) a similar study is shown in the axial-vector channel (χ_{c1}). However, the temperature range is much narrower: $T/T_c = 1.05, 1.08, 1.12, 1.16$ and 1.20. We conclude that this state melts at much lower temperature. In fact, this is a general pattern that we find: S wave states survive to relatively high temperature, while P wave states melt quickly. This has also been observed in the quenched studies.[2)–4),12)]

Maximum Entropy studies at finite temperature are difficult. One way to avoid MEM as much as possible is to use it only at the lowest temperature (with the largest value of N_τ) and use this information to extract information from euclidean correlators at higher temperature. For this we use the standard relation between a euclidean correlator G and spectral function ρ,

$$G(\tau;T) = \int_0^\infty \frac{d\omega}{2\pi} K(\tau,\omega;T)\rho(\omega;T), \qquad K(\tau,\omega;T) = \frac{\cosh[\omega(\tau - 1/2T)]}{\sinh(\omega/2T)}, \quad (2{\cdot}1)$$

where the temperature dependence of the quantities involved is explicitly indicated. The temperature dependence of euclidean correlators arises from two sources: the uninteresting kinematical dependence in the kernel K and the interesting dynamical dependence in the spectral function. The kinematical effect can be eliminated by considering *reconstructed correlators*,[3)] defined by

$$G_{\rm rec}(\tau;T,T_0) = \int_0^\infty \frac{d\omega}{2\pi} K(\tau,\omega;T)\rho(\omega;T_0), \quad (2{\cdot}2)$$

where T_0 is a reference temperature with large N_τ ($= 32$ in our case). Any deviation

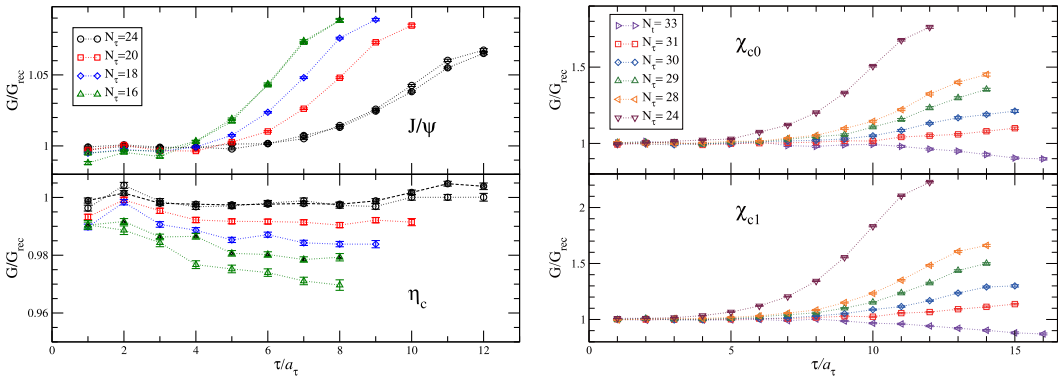

Fig. 3. Ratio of the correlators and reconstructed correlators as a function of euclidean time in the vector and pseudoscalar channel (left) and the scalar and axial-vector channel (right) at different temperatures.

of the ratio $G(\tau;T)/G_{\rm rec}(\tau;T,T_0)$ from 1 will be due to changes in the spectral function (unfortunately the opposite is not true).

In Fig. 3 the ratio of the correlators and reconstructed correlators is shown as a function of euclidean time for the S waves (left) and the P waves (right) for a number of temperatures. While for the S waves the deviation from 1 is only a few percent, even for the highest temperatures considered here, for the P waves the deviation is much large and already present at low temperatures. Both results are consistent with the conclusions drawn from the spectral function analysis, but less reliant on MEM since it is only used at $T/T_c = 1.05$. Also, the ratio is remarkably similar in quenched and dynamical simulations.[3),12)]

§3. Transport

I now move to the low-energy regime in spectral functions, relevant for hydrodynamical evolution in the QGP. As is well-known, Kubo relations relate transport coefficients (shear and bulk viscosity, conductivity, diffusion constants) to current-current spectral functions at vanishing energy. For instance, the electrical conductivity, to be discussed below, is defined as $\sigma = \lim_{\omega\to 0}\rho_{kk}(\omega)/6\omega$, where $\rho_{kk}(\omega)$ is the expectation of the commutator of the EM current $j_k = \bar{\psi}\gamma_k\psi$ at zero momentum.

Again the difficulty is to extract the spectral function, and in particular the low energy behaviour, from euclidean correlators. I now go a bit more in detail.[13)] If $G_E(\tau)$ is determined numerically on a lattice with $N_\tau = 1/aT$ points in the euclidean time direction (a is the temporal lattice spacing), the inversion of Eq. (2·1) is an ill-posed inversion problem, since $G_E(\tau)$ is known at, say, $\mathcal{O}(10)$ data points, whereas $\rho(\omega)$ is needed at $\mathcal{O}(10^3)$ values (after imposing a high-energy cutoff $\omega_{\rm max}$ and discretizing the resulting finite interval $0 < \omega < \omega_{\rm max}$). One possible solution is to provide an Ansatz for the spectral function, with a small number of free parameters. In this case it is important to be able to judge the applicability of the Ansatz. An orthogonal approach is to avoid giving functional forms but only

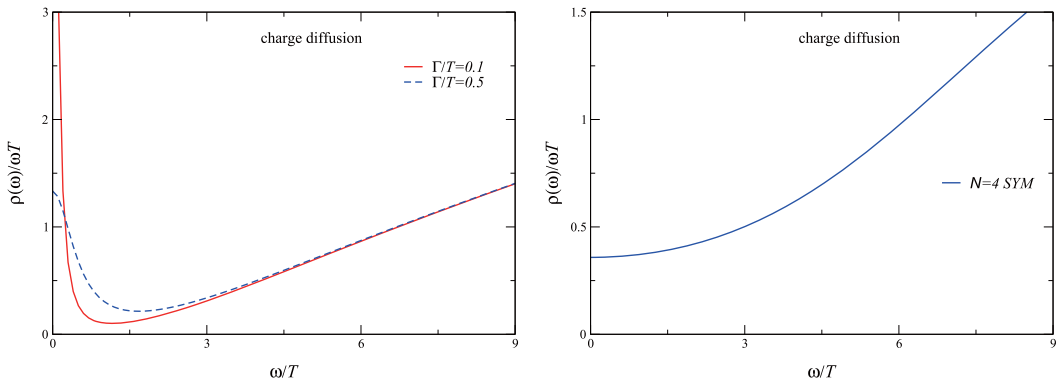

Fig. 4. Current-current spectral function, relevant for electrical conductivity. Left: Sketch based on a weak-coupling analysis, for two values of the collisional width Γ. Right: Analytical result in $\mathcal{N}=4$ SYM at large N_c and 't Hooft coupling, obtained using gauge/gravity duality.

supply a *minimal* amount of prior information, such as positivity ($\omega\rho(\omega) \geq 0$) and asymptotic behaviour ($\rho(\omega) \sim \omega^n$ for large ω). Methods based on this approach are usually collectively referred to as Bayesian techniques.

For a weakly coupled quark-gluon plasma, the extraction of transport coefficients is notoriously difficult, since euclidean correlators are remarkably insensitive to the structure of spectral functions at energies $\omega \ll T$.[14] In Fig. 4 (left) I show a sketch of the spectral function relevant for the conductivity in the hydrodynamic regime at weak and slightly stronger coupling. The interaction strength is parametrized by the collisional width Γ, which behaves as g^4T at weak coupling.[15] At weak coupling the so-called transport peak is high and narrow: in that case the euclidean correlator is sensitive to the area under the curve but not to further details. However, at stronger coupling the transport peak is much broader and the small ω limit is no longer singular. This behaviour is also seen analytically in strongly coupled theories where such calculations are possible. In Fig. 4 (right) the same current-current spectral function is shown in $\mathcal{N}=4$ SYM at strong coupling, calculated in the context of gauge-gravity duality.[16),17] Here the transport peak is completely gone and the spectral function behaves in a smooth manner for small ω. This lack of features is in fact an encouraging sign and opens up the possibility that transport coefficients are accessible in lattice QCD above the deconfinement transition.

So far the number of papers in the literature that have attempted to extract transport coefficients from the lattice in a head-on approach is very small. A first attempt to measure transport coefficients can be found in the pioneering paper by Karsch and Wyld, using an Ansatz.[18] This method was followed by Nakamura and Sakai for the shear and bulk viscosity.[19] For a critical discussion of the Ansatz, see Ref. 14). Gupta used Bayesian methods to isolate the transport contribution at small energies in the case of the electrical conductivity.[20] Recently two significant steps have been made. It was known from previous work that MEM performs poorly at small energies. We have identified and resolved a numerical instability in MEM in the limit that $\omega \to 0$ and applied the new formulation to obtain the electrical

conductivity.[21] This will be discussed below. Precisely determined correlators are essential to have control over the analytical continuation; while for the electrical conductivity this is not a problem, for the shear and bulk viscosity standard measurement techniques are insufficient. Meyer has applied a two-level algorithm to better determine energy-momentum correlators and found a result for the shear[22] and bulk[23] viscosity (see also these proceedings[24]). All calculations to date have been performed in quenched QCD, so one may think of the electrical conductivity in pure gauge theory as representing the transport properties of a single electrically charged quark diffusing through a gluon plasma.

I will now briefly describe the algorithmic progress made by us in the Maximum Entropy Method. In order to obtain $\rho(\omega)$ at $N_\omega = \mathcal{O}(10^3)$ values whereas the correlator is only known at $N = \mathcal{O}(10)$ points, the number of coefficients parametrizing the spectral function has to be reduced and cannot exceed N, or in other words, $\rho(\omega)$ has to be restricted to an (at most) N dimensional subspace. In Bryan's algorithm[25] this is achieved via a singular value decomposition (SVD) of the kernel $K(\omega,\tau)$. Viewed as an $N_\omega \times N$ matrix, the kernel is written as $K = UWV^T$, where U is an $N_\omega \times N$ matrix, with $U^TU = 1_{N\times N}$, W is a diagonal $N \times N$ matrix, and V is an orthogonal $N \times N$ matrix. The N dimensional subspace is spanned by the column vectors of U: $u_i(\omega_n) = U_{ni}$. These basis vectors are orthogonal but not complete.

It turns out that at small energies the basis functions diverge when $\omega \to 0$, although they are normalized. This apparent divergence is due to the singular behaviour of the kernel: in the limit that $\omega \to 0$ one finds that $K(\omega,\tau) = 2T/\omega + \mathcal{O}(\omega/T)$. Note that the leading singular term is τ independent; all τ independence resides in the subleading terms. In actual applications of MEM, we (and others) found irregular behaviour at small ω. Needless to say that this prevents access to the transport properties encoded in euclidean correlators. It is worth pointing out that this problem only appears at finite temperature, since at zero temperature the kernel reduces to $K(\omega,\tau) = e^{-\omega\tau}$ and the limit $\omega \to 0$ is smooth. It is a manifestation of the fact that the limits $\omega \to 0$ and $T \to 0$ do not commute.

Once the problem is identified, it is straightforward to solve it. The $1/\omega$ divergence can be avoided by defining $\overline{K}(\omega,\tau) = (\omega/2T)K(\omega,\tau)$, and $\overline{\rho}(\omega) = (2T/\omega)\rho(\omega)$. Since $K(\omega,\tau)\rho(\omega) = \overline{K}(\omega,\tau)\overline{\rho}(\omega)$, the standard relation with the euclidean correlator holds. However, the modified kernel is finite when $\omega \to 0$: $\overline{K}(0,\tau) = 1$. A SVD of $\overline{K}$ yields new basis functions $\overline{u}_i(\omega)$, which take a finite value when $\omega \to 0$. MEM now reconstructs $\overline{\rho} \sim \rho/\omega$ rather than ρ. This reshuffling of powers of ω is nontrivial, since $\overline{\rho}$ and ρ are not expanded in a complete set: the reduction step restricts $\overline{\rho}$ to a different subspace with different properties, in particular in the small ω limit.

A second (minor) modification is needed to access $\rho(\omega)/\omega$ at zero ω, relevant for transport coefficients. For spectral functions of fermion bilinears, such as $j_\mu = \bar{\psi}\gamma_\mu\psi$, the traditional default model is $\overline{m}(\omega) \sim m(\omega)/\omega \sim \omega$, determined by the high-energy behaviour $\rho(\omega) \sim \omega^2$. Unfortunately, this introduces a bias and puts the intercept equal to zero from the start. To avoid this, one may use $\overline{m}(\omega) \sim (b+\omega)$, where $b > 0$ is a parameter that can be used to assess default model dependence at small ω.

We have applied the modified algorithm to the problem of the electrical conductivity (or charge diffusion) in quenched QCD with light staggered fermions and

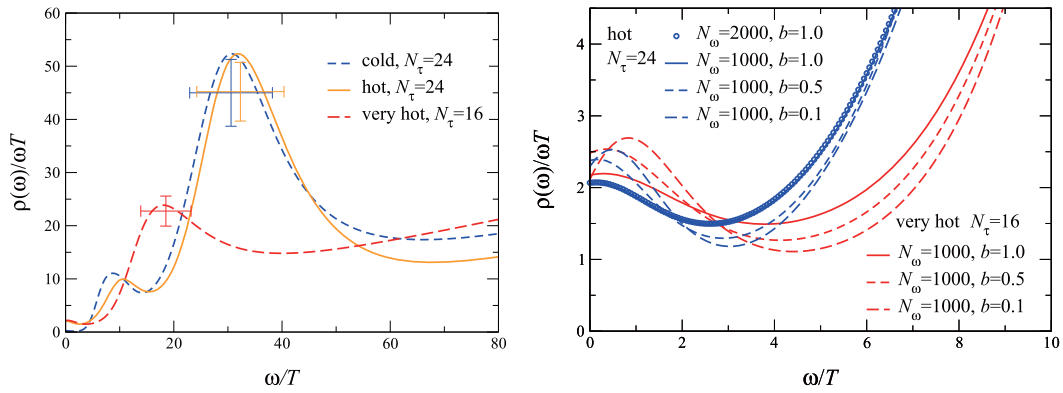

Fig. 5. Current-current spectral function from quenched lattice QCD simulations at T/T_c =0.62 (cold), 1.5 (hot), and 2.25 (very hot) over a large range of ω/T (left) and a blow-up above T_c, indicating sensitivity to MEM parameters. The intercept at $\omega = 0$ is proportional to the conductivity.

performed simulations below the transition on a lattice at $\beta = 6.5$ of size $48^3 \times 24$ and above the deconfinement transition on a finer lattice at $\beta = 7.192$ of size $64^3 \times N_\tau$, with $N_\tau = 24, 16$. The quarks are so light that chiral symmetry restoration is clearly visible when comparing pseudoscalar and scalar correlators.[26] In Fig. 5 (left) the spectral function normalized by ωT is shown for a large range of ω at three temperatures: $T/T_c \sim 0.62$ ($N_\tau = 24$), $T/T_c \sim 1.5$ ($N_\tau = 24$) and $T/T_c \sim 2.25$ ($N_\tau = 16$). A blow-up above T_c is shown in Fig. 5 (right). In this case results for three values of the default model parameter b are shown. The slight spread of the curves gives an indication of the uncertainty in the MEM reconstruction. There is no dependence on the discretization along the ω axis, as can be seen from the results at $N_\tau = 24$ using $N_\omega = 1000$ and 2000 at fixed $\omega_{\rm max}$. From the intercept the conductivity is found to be $\sigma/T = 0.4 \pm 0.1$ with no significant temperature dependence. This result is normalized to a single flavour and should be multiplied with the sum of the electric charge squared for light flavours. The error is systematic and due to the MEM uncertainty. The statistical error is expected to be smaller. This result is indicative of strong interactions: at weak coupling the conductivity behaves as $\sigma/T \sim 1/(g^4 \ln 1/g) \to \infty$, whereas at strong coupling the scale is set solely by the temperature.

§4. Summary

In the recent year some progress on the extraction of spectral functions and transport coefficients from euclidean correlators has been made. I have focused here on the work I was involved in. Clearly, there are many open questions remaining. For instance, Umeda[27] emphasized the role of the constant contribution in the euclidean correlator and how it may obscure the extraction of spectral functions. Concerning potential models, Mocsy and Petreczky have performed a detailed analysis of these and argued that also the S wave states may melt earlier than seen on the lattice.[28]

Finally, Laine et al. have reconsidered the derivation of potential models in thermal field theory and argued for a qualitatively different potential than usually considered, containing an imaginary part.[29),30)]

Acknowledgements

It is a pleasure to thank my Swansea and Trinity colleagues for their collaboration and the organizers of the YITP programme for the splendid introduction to Kyoto and Japan.

References

1) G. Aarts, PoS(LATTICE 2007)001; arXiv:0710.0739.
2) M. Asakawa and T. Hatsuda, Phys. Rev. Lett. **92** (2004), 012001; hep-lat/0308034.
3) S. Datta, F. Karsch, P. Petreczky and I. Wetzorke, Phys. Rev. D **69** (2004), 094507; hep-lat/0312037.
4) T. Umeda, K. Nomura and H. Matsufuru, Eur. Phys. J. C **39S1** (2005), 9; hep-lat/0211003.
5) G. Aarts, C. Allton, M. B. Oktay, M. Peardon and J. I. Skullerud, Phys. Rev. D **76** (2007), 094513; arXiv:0705.2198.
6) D. B. Kaplan, Phys. Lett. B **288** (1992), 342; hep-lat/9206013.
7) C. Allton et al. (RBC and UKQCD Collaborations), Phys. Rev. D **76** (2007), 014504; hep-lat/0701013.
8) G. Aarts and J. Foley (UKQCD Collaboration), J. High Energy Phys. **02** (2007), 062; hep-lat/0612007.
9) F. Karsch, E. Laermann, P. Petreczky and S. Stickan, Phys. Rev. D **68** (2003), 014504; hep-lat/0303017.
10) G. Aarts and J. M. Martínez Resco, Nucl. Phys. B **726** (2005), 93; hep-lat/0507004.
11) R. Morrin, A. O. Cais, M. Peardon, S. M. Ryan and J. I. Skullerud, Phys. Rev. D **74** (2006), 014505; hep-lat/0604021.
12) A. Jakovac, P. Petreczky, K. Petrov and A. Velytsky, Phys. Rev. D **75** (2007), 014506; hep-lat/0611017.
13) M. Asakawa, T. Hatsuda and Y. Nakahara, Prog. Part. Nucl. Phys. **46** (2001), 459; hep-lat/0011040.
14) G. Aarts and J. M. Martínez Resco, J. High Energy Phys. **04** (2002), 053; hep-ph/0203177; Nucl. Phys. B (Proc. Suppl.) **119** (2003), 505; hep-lat/0209033.
15) P. Arnold, G. D. Moore and L. G. Yaffe, J. High Energy Phys. **11** (2000), 001; hep-ph/0010177; J. High Energy Phys. **05** (2003), 051; hep-ph/0302165.
16) D. Teaney, Phys. Rev. D **74** (2006), 045025; hep-ph/0602044.
17) R. C. Myers, A. O. Starinets and R. M. Thomson, J. High Energy Phys. **11** (2007), 091; arXiv:0706.0162.
18) F. Karsch and H. W. Wyld, Phys. Rev. D **35** (1987), 2518.
19) A. Nakamura and S. Sakai, Phys. Rev. Lett. **94** (2005), 072305; hep-lat/0406009.
20) S. Gupta, Phys. Lett. B **597** (2004), 57; hep-lat/0301006.
21) G. Aarts, C. Allton, J. Foley, S. Hands and S. Kim, Phys. Rev. Lett. **99** (2007), 022002; hep-lat/0703008.
22) H. B. Meyer, Phys. Rev. D **76** (2007), 101701; arXiv:0704.1801.
23) H. B. Meyer, Phys. Rev. Lett. **100** (2008), 162001; arXiv:0710.3717.
24) H. B. Meyer, arXiv:0805.4567.
25) R. K. Bryan, Eur. Biophys. J. **18** (1990), 165.
26) G. Aarts, C. Allton, J. Foley, S. Hands and S. Kim, Nucl. Phys. A **785** (2007), 202; hep-lat/0607012.
27) T. Umeda, Phys. Rev. D **75** (2007), 094502; hep-lat/0701005.
28) A. Mocsy and P. Petreczky, Phys. Rev. Lett. **99** (2007), 211602; arXiv:0706.2183.
29) M. Laine, O. Philipsen, P. Romatschke and M. Tassler, J. High Energy Phys. **03** (2007), 054; hep-ph/0611300.
30) M. Laine, J. High Energy Phys. **05** (2007), 028; arXiv:0704.1720.